Effects of Traffic Load Amplitude Sequence on the Cracking Performance of Asphalt Pavement with a Semi-rigid Base

Linyi Yao[a], Zhen Leng[a,*], Jiwang Jiang[a,b], Chenze Fang[c], Fujian Ni[b]

[a] *Department of Civil and Environmental Engineering, The Hong Kong Polytechnic University, Hung Hom, Kowloon, Hong Kong*

[b] *Department of Highway and Railway Engineering, School of Transportation, Southeast University, Nanjing, Jiangsu, China*

[c] *Department of Transportation Engineering, Dalian Maritime University, Dalian, Liaoning, China*

*corresponding author

Email: zhen.leng@polyu.edu.hk

Effects of Traffic Load Amplitude Sequence on the Cracking Performance of Asphalt Pavement with a Semi-rigid Base

The propagation of cracks in in-service asphalt pavements is closely related to the complicated traffic loading patterns over time. However, typical traffic-related variables capture only the overall traffic level without being able to account for the load-time history. Therefore, this study aims to investigate the effects of traffic load sequence on the cracking performance of asphalt pavement from both field and laboratory perspectives. A load amplitude sequence (LAS) index was developed to characterize the traffic loading sequence in the field. Two machine learning (ML) algorithms, namely artificial neural network (ANN) and random forest regression (RFR), were applied to correlate the LAS index with field pavement cracking performance. The two-block semi-circular bending (SCB) test was developed to characterize the non-linear fatigue damage accumulation of asphalt mixtures. It was found that heavier traffic loads in early stages are detrimental to the long-term pavement cracking performance. The LAS index plays a crucial role in the prediction and development of pavement cracks. The laboratory test results reveal that a loading sequence starting with a higher stress may shorten the fatigue life and vice versa. The outcomes of this study may contribute to a better understanding of the traffic loading characterization of in-service asphalt pavements.

Keywords: Load amplitude sequence, Pavement cracking, Traffic loading characterization, Machine learning, Variable amplitude fatigue test.

1 Introduction

The semi-rigid base asphalt pavement, consisting of one or more asphalt layers on a cement-treated base, is the main type of pavement structure in China since 1997 (Dong *et al.*, 2021). Compared with conventional flexible pavement, the cement-treated materials in semi-rigid base asphalt pavement could effectively reduce the vertical compressive strain on the subgrade and enhance the bearing capacity of the road structure (Zang *et al.*, 2018). However, asphalt pavement with a semi-rigid base is prone to generate transverse cracks due to temperature variation, cycling traffic loading and reflection from the base layer. As a result, periodic maintenance and rehabilitation (M&R) treatments are required to maintain the functionality of the pavement, which incur vast maintenance costs and significant environmental burdens (Santos *et al.*, 2017; Hu *et al.*, 2019). Therefore, it is necessary to examine the influence of different factors, such as material properties and climate and traffic conditions (Abaza, 2016), on the deterioration of pavement cracking performance.

In terms of traffic, equivalent single axle load (ESAL) is commonly used for characterizing the traffic load conditions of a road segment. It has been often employed as an important traffic input for pavement design (AASHTO, 1993) and as a key influencing factor for pavement performance prediction (Yao *et al.*, 2019; Guo *et al.*, 2021). Damage caused by wheel loads of varying magnitudes and repetitions is converted to damage from an equivalent number of standard loads by ESAL. It depicts a mixed stream of traffic accumulated over the analysis period with various axle loads and axle configurations. However, the accuracy of the ESAL expression has long been debated by pavement experts (Prozzi and Madanat, 2004; Guler and Madanat, 2011). To avoid the errors caused by ESAL conversion, some studies directly used the information from the entire axle load spectrum, such as the proportion, magnitude and repetitions of loads in each axle load group, to characterize the traffic load condition (Timm *et al.*, 2005; Haider and Harichandran, 2009). Although many researchers have claimed the importance of ESAL and axle load spectrum in predicting pavement performance (Solatifar and Lavasani, 2020; Yao *et al.*, 2020; Tran and Hall, 2007), both measures can only capture the overall traffic level of a road section. ESAL is calculated by summing up the equivalent axle loads over the analysis period, whereas variables extracted from the axle load spectrum depict the overall distribution of axle loads in various weight ranges. Neither of them has taken into account the traffic loading history over a certain period of time, but some studies have reported the impact of loading sequences on the performance deterioration of asphalt mixtures (Jiang *et al.*, 2016).

Moreover, field observations show that asphalt pavements with similar ESAL or axle load spectrum in the same climate zone can have significantly distinct degradation rates, resulting in different maintenance needs. The early damage of asphalt pavement is also considered to be closely related to the traffic overload phenomenon at the beginning of the service life (Pais *et al.*, 2013). Both phenomena are very likely to be caused by the different traffic loading histories. Therefore, in addition to the overall traffic level, other factors associated with the traffic loading history, such as the time series of load amplitudes, are also potential contributing factors to the deterioration of asphalt pavements.

Most laboratory tests for testing the performance of asphalt mixture were developed based on cyclic loading with single amplitude, frequency and waveform (Benedetto *et al.*, 2011; Wang *et al.*, 2022), which can hardly reflect the complex loading sequence effects. Considering the complex and almost stochastic loading conditions of in-service pavements, it would be useful to understand the deterioration of pavement cracking performance under variable-amplitude loading, which has been well applied to characterize the fatigue cracking propagation in other materials and structures (Zhu *et al.*, 2019; Yuan *et al.*, 2015). At present, several incremental dynamic loading tests are available to simulate the multiple load amplitude conditions in the field, such as the Incremental Repeated Load Permanent Deformation (iRLPD) test (Azari and Mohseni, 2013), Multi-sequenced Repeated Load (MSRL) test (Dong *et al.*, 2018), and Triaxial Stress Sweep (TSS) test (Kim and Kim, 2017). They introduced load amplitude sequences into laboratory tests for characterizing the rutting resistance of asphalt mixtures (Azari and Mohseni, 2021; Zhao *et al.*, 2020; Wang *et al.*, 2018). The creep accumulation process in asphalt mixtures at high temperatures depends on the time history of the applied stress/strain. However, for intermediate temperatures, there is still little field or laboratory validation for the impact of loading sequences on the development and propagation of cracks in asphalt pavements. The load amplitude sequence was also rarely considered in the performance model of asphalt pavements.

To fill the aforementioned knowledge gap, this study aims to investigate the effects of traffic load amplitude sequence on the cracking performance of semi-rigid base asphalt pavement from both field and laboratory perspectives. A new Load Amplitude Sequence (LAS) index is proposed, which is expected to compensate for the traditional traffic variables, allowing for more accurate pavement performance prediction and improved maintenance planning.

2 Data and Material Preparation

2.1 Field data collection

The Pavement Management System (PMS) in Jiangsu, China has a databased with a large amount of field data for over 14,000 lane kilometers of highway. These data cover information related to pavement structures and materials, traffic loads, climate conditions, pavement performance, and maintenance history for each expressway. The time span of these data ranges from 2003 to 2021, providing sufficient data support for the smooth running of the research. Prior to analysis, each expressway was divided into sub-sections based on the location (pavement or bridge), lanes, directions, and the structural and traffic sections to which they belong. Subsections longer than 1.5 km were further subdivided at 1 km intervals. After excluding some segments with incomplete information or very short length, a total of 10,330 pavement segments were obtained, totaling 8,771 lane kilometers.

2.2 Selection of influential factors and pavement cracking index

Transverse cracking is the most prevalent forms of cracking on asphalt pavement with a semi-rigid base, accounting for more than 85% of all distress (Zhou *et al.*, 2014). Thus, in this study, the Transverse Cracks Evaluation Index (TCEI) proposed in (Zhou *et al.*, 2010) was used to assess the cracking performance of semi-rigid base asphalt pavements. The TCEI was derived by converting the ratio of Transverse Crack Spacing (TCS) to transverse crack width ratio (TWR) to a scale of 0 to 100, with 100 being the intact condition (i.e., no transverse cracks). The influential factors for constructing the cracking performance model were identified by reviewing the relevant literature (Yao *et al.*, 2021; Karlaftis and Badr, 2015) and checking the availability of information in the PMS. Particularly, the

LAS index was proposed to approximately describe the evolution of field load amplitudes during a given analysis period. The detailed definition of LAS will be introduced later. PLDF (Proxy of Lane Distribution Factor) is a nominal variable, combining the number of lanes (4, 6, or 8) in the current section with the index of the current lane (1, 2, 3, or 4). It was used to represent the lane distribution factor, indicating how traffic is distributed in different lanes. Table 1 summarizes the influencing factors considered in this study.

Table 1 The selected influential factors and pavement cracking index.

Class	Variables	Description	Unit or magnitude
Pavement structures and materials	SBS modified asphalt layer thickness	The thickness of Styrene-Butadiene-Styrene (SBS) modified asphalt layers	cm
	Asphalt layer thickness	The total thickness of all asphalt layers	cm
	Asphalt layer material	The gradations of the multiple asphalt layers	/
	Base layer thickness	The thickness of base course	cm
	Base layer material	The material of base course	/
Traffic loads	ESAL	The equivalent single-axle loads	$\times 10^4$
	Overload rate	The percentage of overweight axle loads to total axle loads	dimensionless
	LAS	The load amplitude sequence index proposed in this study	dimensionless
Climate factors	R_over 35 °C	Proportion of days with daily maximum temperature over 35 °C	%
	R_below 0 °C	Proportion of days with daily minimum temperature below 0 °C	%
	Ratio of rainy days	Proportion of rainy days	%
	Mean temperature	The daily average air temperature	°C
	Mean precipitation	The daily average precipitation	mm
Performance	TCEI	Transverse Cracks Evaluation Index	dimensionless
Others	PLDF	The combination of the number of lanes in the current section and the index of the current lane	/
	Road or bridge	Whether it is a bridge pavement or a road pavement	/
	Service time	The interval from the time when the road section was opened to traffic to the time	year

	of the current pavement inspection

2.3 *Materials and mixture design*

To further verify the loading sequence effect on asphalt mixtures, a commonly used stone mastic asphalt (SMA) mixture with a nominal aggregate size of 10mm and aggregate type of granite was selected for the research. SBS modified asphalt binder with Superpave performance grade of 76-16 (PG76-16) and optimum content of 6.0% by weight of asphalt mixture was used. The target air void content was 4±0.5%. The detailed aggregate gradation is shown in Figure 1. The loose mix was first subjected to a long-term oven aging procedure at 135 ºC for 8 h (Chen *et al.*, 2021). Then, the aged loose mix was compacted into cylindrical specimens with diameters and heights of 150 mm using the Superpave Gyratory Compactor (SGC). Following that, around 20 mm were removed from both ends of each cylindrical specimen due to a considerably larger air void content as compared to the central region. Finally, the remaining middle part of each cylindrical specimen was cut into four half rings with a diameter of 150 mm and a height of 50 mm, as shown in Figure 2(a). All half ring specimens were measured for air void content, and those with air void content outside the range of 4±0.5% were discarded. As Figure 2(b) shows, the qualified half ring specimens were selected for the semi-circular bending (SCB) test under different load conditions.

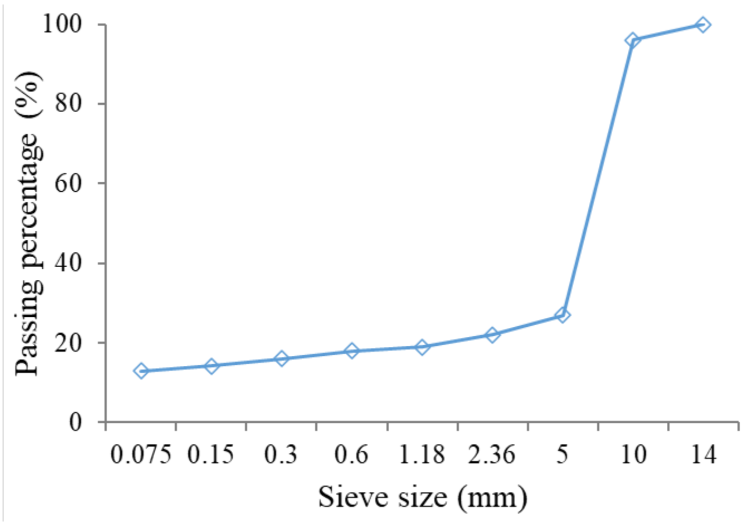

Figure 1. Aggregate gradation.

(a) (b)

Figure 2. Specimen preparation: (a) half ring specimens; (b) set-up of the SCB test.

3 Methodology

An overview of the methodology used in the present study is shown in Figure 3. The effect of traffic load amplitude sequence on asphalt pavement cracking were investigated from both field and laboratory perspectives. Field validation started from collecting field data, selecting influential factors, and defining load amplitude sequence (LAS) index. Armed with this information, the deterioration of pavement cracking condition at different LAS levels was first graphically displayed to show the presence of the loading sequence impact on pavement cracking. Then, two machine learning (ML) models were developed to model the correlation between the LAS index and TCEI. Finally, for the superior model, an in-depth interpretation and analysis of the model output would be performed to further examine the effect of loading sequence on pavement cracking and its interaction with other factors. Laboratory validation was achieved by conducting two-block SCB tests to characterize the nonlinear damage accumulation in asphalt mixture under different loading conditions. To do so, SCB specimens were first prepared and loading sequences with constant and variable amplitudes were designed accordingly. Based on this, the fatigue curves and fatigue damage parameters of asphalt mixtures under different loading conditions were obtained and compared. The laboratory test results are expected to provide a better understanding of the underlying physical meaning of the LAS index.

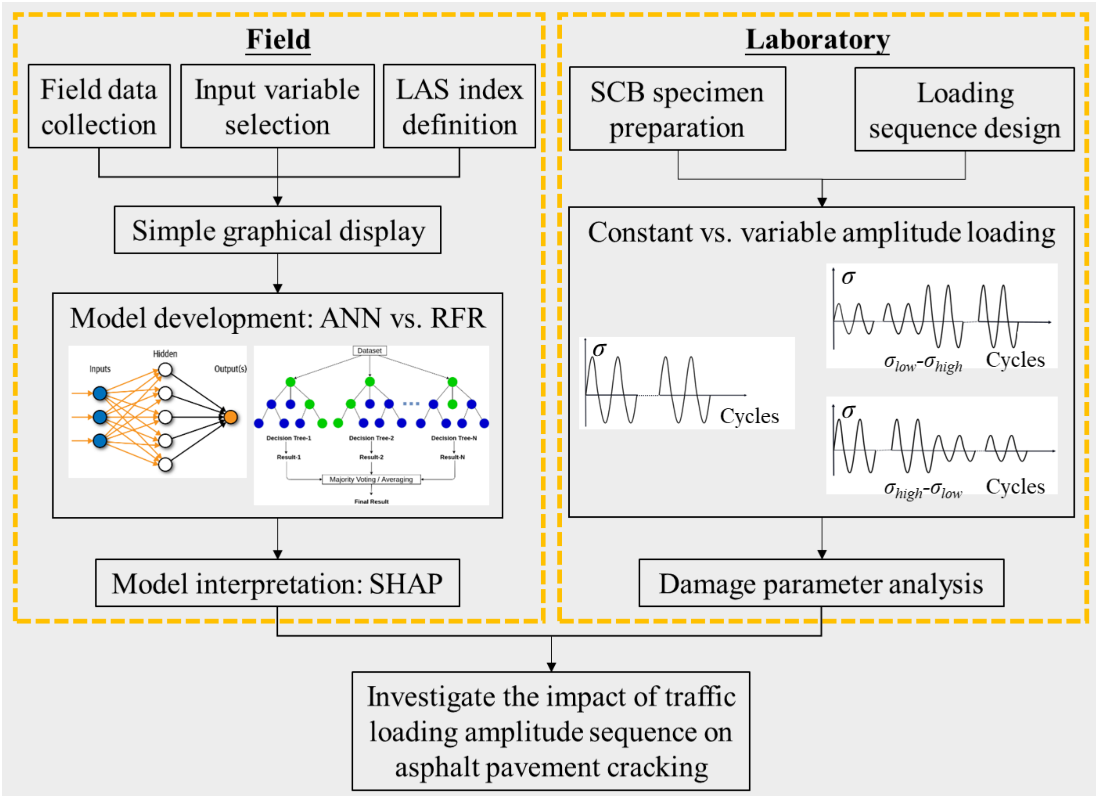

Figure 3. Overview of the methodology adopted in the present study.

3.1 Field validation

3.1.1 Load amplitude sequence index

To capture the characteristics of traffic load amplitude sequence in the field, the LAS index was proposed in this study. It was developed based on the variation of overload rate of the vehicle axle during a specific period. Overloading of large and medium-sized trucks was very common on the highways in Jiangsu, especially in the early years, causing a lot of early damage to the pavement structure. According to the regulations issued by the Ministry of Transport of the People's Republic of China (Ministry of Transport of the People's Republic of China, 2016), the axle limits for single-, tandem- and tridem-axle double-wheel set are 10, 18 and 22 tonnes, respectively. Based on this, Eq. 1 gives the formula for determining the LAS index for a certain pavement section:

$$LAS = R_{overload}\left(T_{half}\right)/R_{overload}(T) \tag{1a}$$

$$R_{overload}(t) = \sum_{a\in A}\sum_{t'=0}^{t} n_{a,t'}^{overload} / \sum_{a\in A}\sum_{t'=0}^{t} n_{a,t'}^{tot} \tag{1b}$$

$$\mathrm{A} = \{\mathrm{single, tandem, tridem}\} \tag{1c}$$

$$f: ESAL \rightarrow t \tag{1d}$$

$$T = f(ESAL_{end}) \tag{1e}$$

$$T_{half} = f(ESAL_{end}/2) \tag{1f}$$

where $R_{overload}(t)$ = the overload rate during the time period of 0 to t; a = a specific axle type, $a \in A$; A = the set of axle types; $n_{a,t'}^{overload}$ = the number of overloaded axles of axle type a at time t'; $n_{a,t'}^{tot}$ = the total number of axles of axle type a at time t'; f = a mapping from $ESAL$ to time t; $ESAL_{end}$ = the ESAL at the end point of the calculation range; T = the time at the end of the calculation range; T_{half} = the time when ESAL is equal to half of the ESAL at the end point of the calculation range.

Essentially, the LAS index is the ratio of the overload rate for the first half of ESALs to the total overload rate for all ESALs. A simple rule is that LAS index less than one corresponds to the case where the traffic load is first light and then heavy, and vice versa. In addition, LAS index can be calculated for various calculation ranges, which allows to investigate the loading sequence effect on pavement cracking performance at different service stages.

3.1.2 Modelling of field data

To explore the effect of load amplitude sequence on pavement cracking from massive and multi-source field data, two popular ML algorithms, artificial neural network (ANN) and random forest regression (RFR), were applied for modelling the relationships between the LAS index and other selected influential factors with TCEI.

ANN models have been extensively used for pavement performance prediction because of their effectiveness in handling complex nonlinear relationships (Yao *et al.*, 2019; Guo *et al.*, 2021). These models are typically composed of many artificial neurons that are mutually connected. The connections are referred to as parameters or weights, reflecting the learnt knowledge from a dataset. Back-propagation was employed to train the ANN model which fine-tunes the parameters of the neural network depending on error rates acquired in each iteration. The optimum hyper-parameters in this study were determined through a simple grid search method which builds a model for every specified hyper-parameter combination and compares the performance of each model. The entire dataset was randomly divided into two groups: 80% for training and 20% for testing (Gholamy *et al.*, 2018). The mean squared error (MSE) was chosen as the loss function. The ANN model was built and tested on PyTorch, a well-known deep learning framework in Python (Van Rossum and Drake, 2009).

Random Forest (RF) is an ensemble technique that uses multiple decision trees to solve both regression and classification problems. It utilizes bagging and feature randomness in the creation of each individual tree in an attempt to generate an uncorrelated forest of trees whose prediction is more accurate than that of any individual tree. Therefore, RF is usually less likely to be over-fitting. In this study, the application of RFR algorithm was performed using the scikit-learn package in Python (Pedregosa *et al.*, 2011). The optimum set of hyper-parameters was found through random search which creates a grid of hyper-parameter values and picks random combinations to train and assess the model. This process was completed using the *RandomizedSearchCV* function in scikit-learn.

3.1.3 Model interpretation

The ML models were interpreted through the SHapley Additive exPlanations (SHAP) approach, which is a game-theoretic technique for explaining the output of any ML model (Lundberg and Lee, 2017). It is a unified framework for explanation models using additive feature attribution methods. SHAP specifies the explanation model as:

$$g(z') = \phi_0 + \sum_{i=1}^{M} \phi_i z_i' \tag{2}$$

where g is the explanation model, ϕ_0 is the model output with all inputs absent which can be approximated by the average model predictions, $z' \in \{0,1\}^M$ is the simplified features, M is the number of simplified input features, and ϕ_i is the feature attribution for a feature i, i.e., the SHAP values. The SHAP value is computed by averaging the changes in conditional expectations over all possible feature orderings (Lundberg and Lee, 2017). It represents the responsibility of a feature for a change in the model output. In this study, the Python SHAP library was used to apply the SHAP method so as to explain the effect of loading amplitude sequence on the cracking performance of in-service asphalt pavements.

3.2 Two-block SCB test

The setup of the two-block SCB test includes a loading ramp at the top center of the specimen, and two support rollers on the bottom sides with a spacing of 120 mm, which was 0.8 times the diameter of the asphalt mixture specimen. Two pre-tests, SCB strength test and SCB constant amplitude fatigue test (Jiang *et al.*, 2018), were first conducted to determine the strength and fatigue life of the asphalt mixture under a single load amplitude, respectively. The SCB strength test was carried out under a constant pre-defined displacement rate of 50mm/min at room temperature of 25ºC. Three replicated specimens were tested to obtain the load-displacement curves and the corresponding mean value and coefficient of variable (COV) of the tensile strength were calculated according to Eq. 3 and shown in Table 2. As for the SCB constant amplitude fatigue test, the loading frequency was determined to be 10Hz with haversine waveform. One low stress ratio (σ_{low}) of 0.135 and one high stress ratio (σ_{high}) of 0.190 were selected for testing. Three replicates were prepared for both testing conditions and the corresponding fatigue lives of the asphalt mixture are also exhibited in Table 2.

$$\sigma_{max} = \frac{4.976F_{max}}{BD} \quad (3)$$

where σ_{max} = the tensile strength of specimen (MPa); F_{max} = the peak load of specimen (N); B = the height of specimen (mm); and D = the diameter of specimen (mm).

Table 2 Testing results of the SCB strength test and SCB constant amplitude fatigue test.

Tensile Strength (MPa)		Stress ratio	Stress amplitude (MPa)	Fatigue life (Cycles)	
Mean	COV			Mean	COV
5.321	9.0%	0.135	0.718	56,722	6.1%
		0.190	1.011	18,502	12.9%

Two different loading sequences were considered for the two-block SCB tests, one from low to high stress ratios (σ_{low}-σ_{high}) and the other in the opposite direction (σ_{high}-σ_{low}). The loading sequence and waveform settings are the same as those of the SCB constant amplitude fatigue test. The cyclic loading number of the first block was 30% of the fatigue life of the asphalt mixture obtained from the SCB constant amplitude fatigue test. In the second block, the specimen was continuously loaded until fatigue failure. Three replicates were tests for each loading sequence.

4 Results and Discussion

4.1 Field validation

4.1.1 Graphical display of the loading sequence effect

Although the LAS index can be calculated for different service stages, this study aims to explore the long-term effect of loading sequence on pavement cracking performance. Meanwhile, it is believed that the loading sequence effect would become obvious only after a relatively long period of service. Therefore, only calculation ranges of more than 10 years were considered in the subsequent modelling process. In other words, pavement segments that have been maintained before the tenth year or that have been in service for less than ten years were excluded. For segments with more than ten years of service, the time at the end of the calculation range need to be outside the tenth year. Figure 4 shows the distribution of the LAS index. It is obvious that a considerable percentage of the pavement segments have a higher overload rate in the early years, resulting in a LAS index greater than one. This is consistent with the situation in Jiangsu, where the overload rate was initially high but was later effectively controlled, resulting in a reduction in the overload rate.

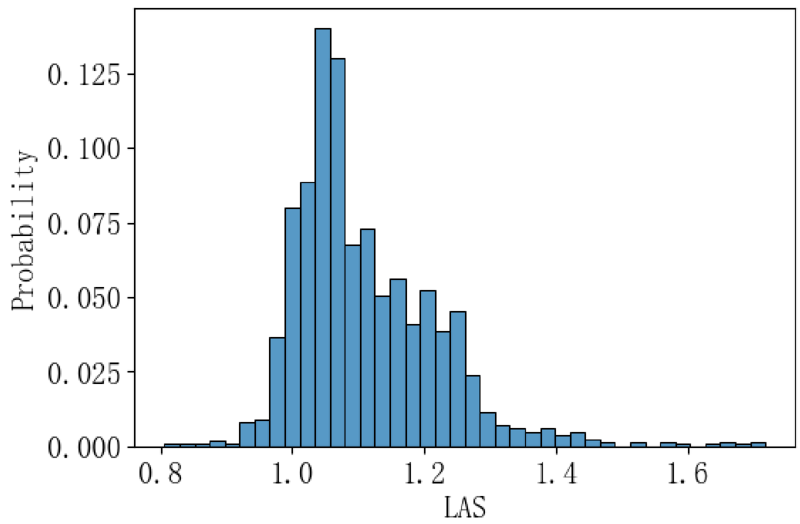

Figure 4. Distribution of the LAS index.

A graphical display of the loading sequence effect on pavement cracking propagation was provided in Figure 5. Figure 5(a) shows the calculated LAS index considering the range of ESAL from 0 to 5-10 million (i.e., the ESAL at the end point of the calculation range is between 5-10 million) while Figure 5(b) is for the range of ESAL from 0 to 10-15 million. The top half of Figure 5(a) and (b) displays the deterioration of pavement cracking condition with ESAL for different LAS groups. The box plots were used to illustrate the TECI distribution for each ESAL and LAS combination, which allows for multi-dimensional comparisons such as mean (the diamond symbol), median (the horizontal line in the box) and variation (the height of the box). The total length of the pavement segments corresponding to each combination of ESAL and LAS is presented in the bottom of Figure 5(a) and (b), implying the sample size utilized to support the results. It can be observed that a larger LAS value tends to increase the TCEI deterioration rate. This suggests that different load amplitude sequences do have an effect on asphalt pavement cracking, which motivated the further analysis of the contribution of the LAS index to pavement cracking through advanced ML modeling and interpretation techniques afterwards.

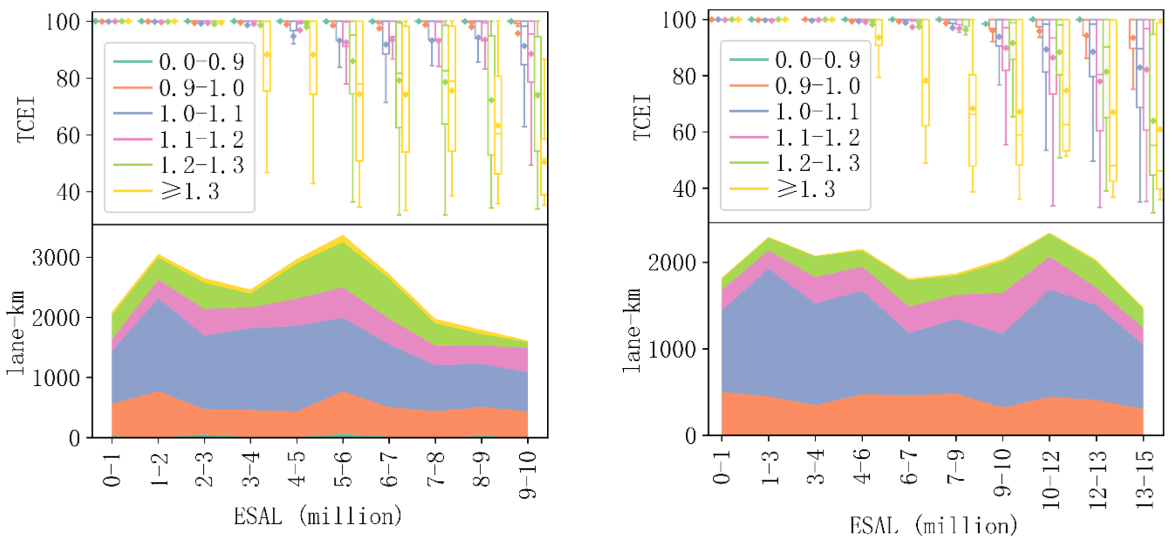

(a) (b)

Figure 5. Deterioration of pavement cracking condition for different LAS values and calculation ranges: (a) in the range of ESAL from 0 to 5-10 million and (b) in the range of ESAL from 0 to 10-15 million.

4.1.2 Importance of LAS in pavement cracking prediction

To examine the importance of LAS in pavement cracking prediction, the accuracy of the prediction models built based on the two ML algorithms were assessed first. Three metrics, including the coefficients of determination (R-square), mean absolute error (MAE), and root mean square error (RMSE), were employed, as shown in Table 3. The R-square values of the two models with LAS reached above 0.85 on the training set and exceeded 0.76 on the test set. The scatter plots in Figure 6 indicate that the majority of the points are densely distributed around the line of equality, which represents the most ideal condition, i.e., the predicted results are exactly equal to the measured results. Therefore, it can be concluded that both models have relatively high accuracy and are able to model the relationship between pavement cracking condition and load amplitude sequence and other factors very well.

Moreover, two more models excluding the LAS index but including all other factors were developed. The evaluation results are also shown in Table 3. It can be found that the performances of both ANN and RFR models are slightly improved after adding the LAS index. Therefore, LAS has a certain contribution to the prediction of pavement cracking. In addition, the RFR model slightly outperforms the ANN model. Hence, in the subsequent analysis, the results of the RFR model were interpreted to examine the effect of loading sequence on pavement cracking.

Table 3 Model evaluation results.

Dataset	Evaluation metrics	ANN			RFR		
		Without LAS	With LAS	Improvement (%)	Without LAS	With LAS	Improvement (%)
Training	R-square	0.8442	0.8541	1.17	0.8813	0.8836	0.26
	MAE	5.4839	5.2891	3.55	4.6660	4.6029	1.35
	RMSE	7.7317	7.4820	3.23	6.7494	6.6847	0.96
	Sample size	6895					
Testing	R-square	0.7495	0.7517	0.29	0.7902	0.7916	0.18
	MAE	7.2086	7.1888	0.27	6.3703	6.3240	0.73
	RMSE	9.8510	9.8073	0.45	9.0133	8.9835	0.33
	Sample size	1700					

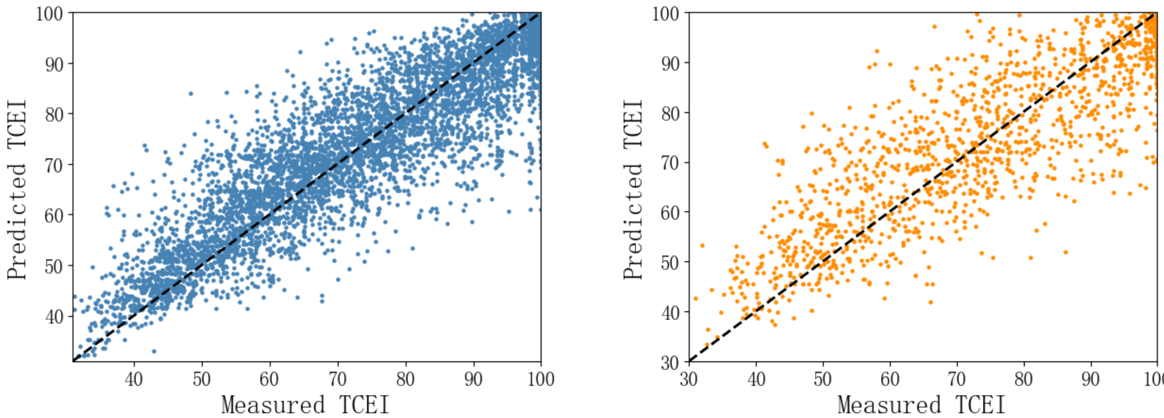

(a) (b)

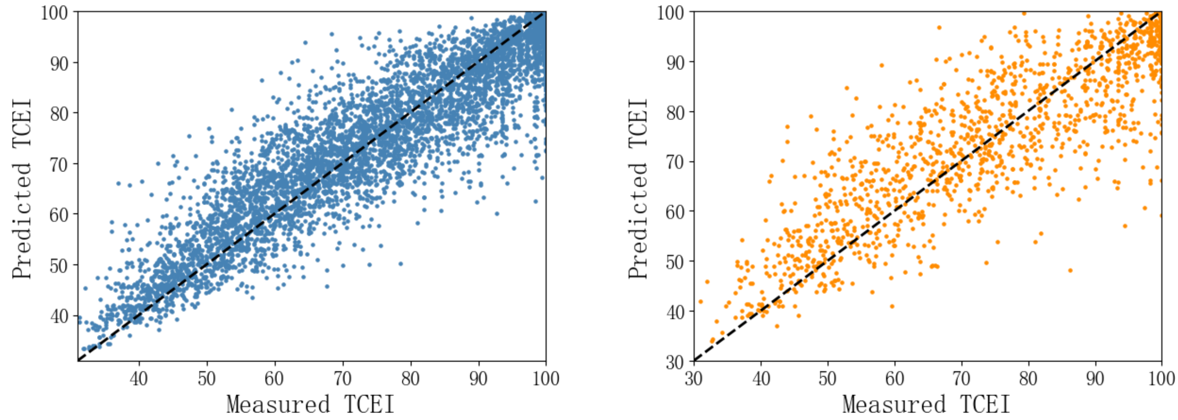

(c) (d)

Figure 6. Measured against predicted TCEI values: (a) training data of ANN model, (b) testing data of ANN model, (c) training data of RFR model, and (d) testing data of RFR model.

SHAP estimates the global importance of a feature as the average of the absolute SHAP values for each feature across the data. The higher the mean absolute value of SHAP, the more important the variable is. Figure 7 normalizes the SHAP values by calculating the percentage of the mean absolute SHAP values for each feature. The features are ranked from the most important to the least important. As can be seen in Figure 7, the location of the pavement (road or bridge) and the structural and material properties of the asphalt pavement layer have the greatest influence on the long-term pavement cracking performance. This is because reflective cracking is one of the major distresses of semi-rigid base asphalt pavements. Hence, road pavements with semi-rigid base usually have more transverse cracks than bridge pavements with steel or concrete deck base. The performance of asphalt layers also significantly affects the speed of upward propagation of transverse cracks. Among the three traffic-related indicators, the LAS index contributed the most in forecasting long-term pavement cracking conditions, even more than the common traffic indicators such as ESAL and overload rate. This demonstrates the importance of including loading sequence metrics in pavement performance models.

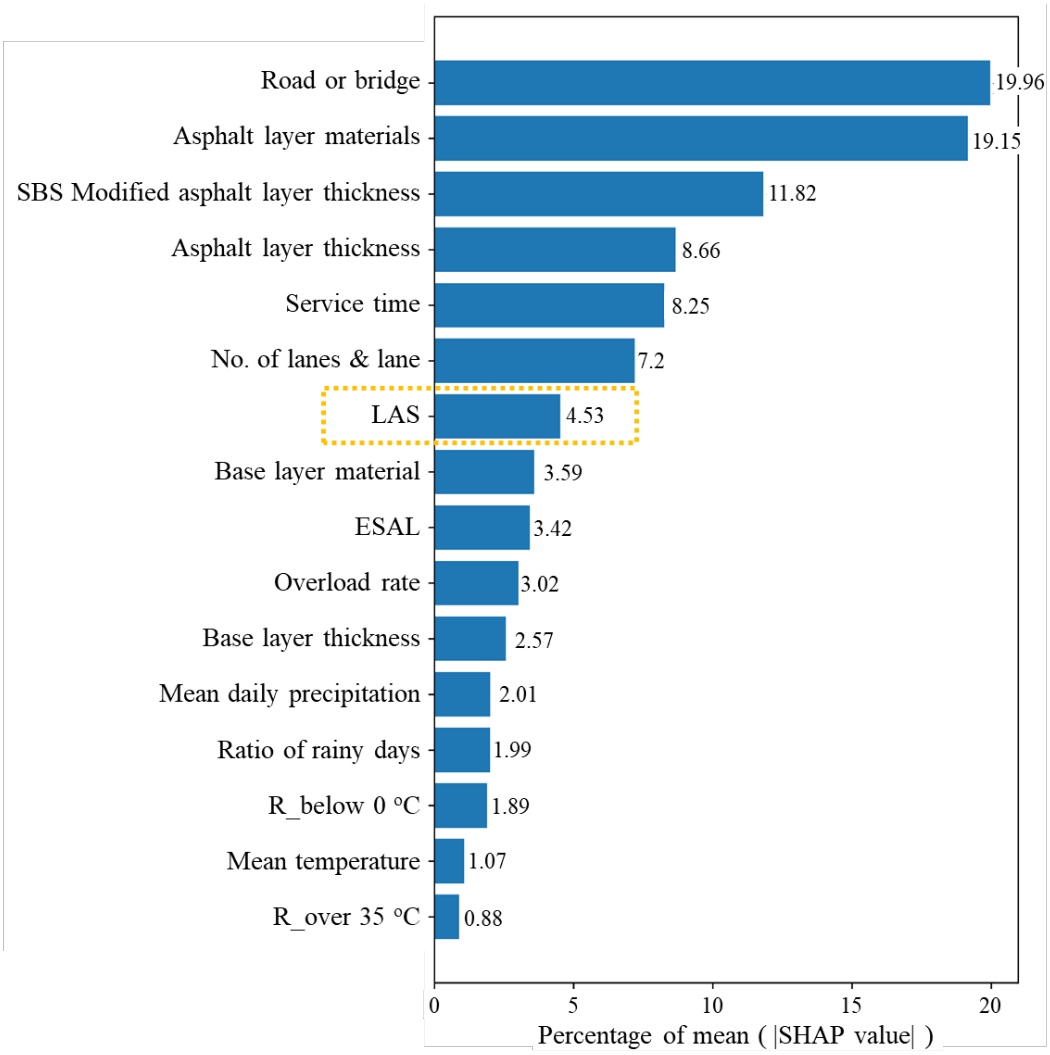

Figure 7. SHAP importance plot.

4.1.3 The effect of LAS on pavement cracking condition

Figure 8 depicts the SHAP values of every feature for every data sample, where the features are ranked from top to bottom according to their importance. The position of the point on the horizontal axis is determined by the SHAP value, and the colour represents the value of the feature, with red being high and blue being low. The SHAP value could be regarded as the marginal contribution of every feature for every data sample. Thus, Figure 8 illustrates how different values of each feature would affect the model output. For example, a thicker SBS modified asphalt layer increases the predicted TCEI value, which corresponds to a milder cracking condition. Moreover, a higher LAS index lowers the predicted

TCEI value, i.e., the traffic load of first heavy and then light will aggravate pavement cracking. Conversely, a light-to-heavy loading sequence prolongs pavement service life. This provides a basis for transport agencies to develop vehicle load limit policies, especially for newly built or maintained road pavements. Meanwhile, Figure 8 also indicates that after ten years of pavement service, the negative effects of heavy ESALs and overload rates on pavement cracking become insignificant, but the negative effects of large LAS values are quite obvious. This also emphasizes the importance of including loading sequences in long-term pavement performance predictions.

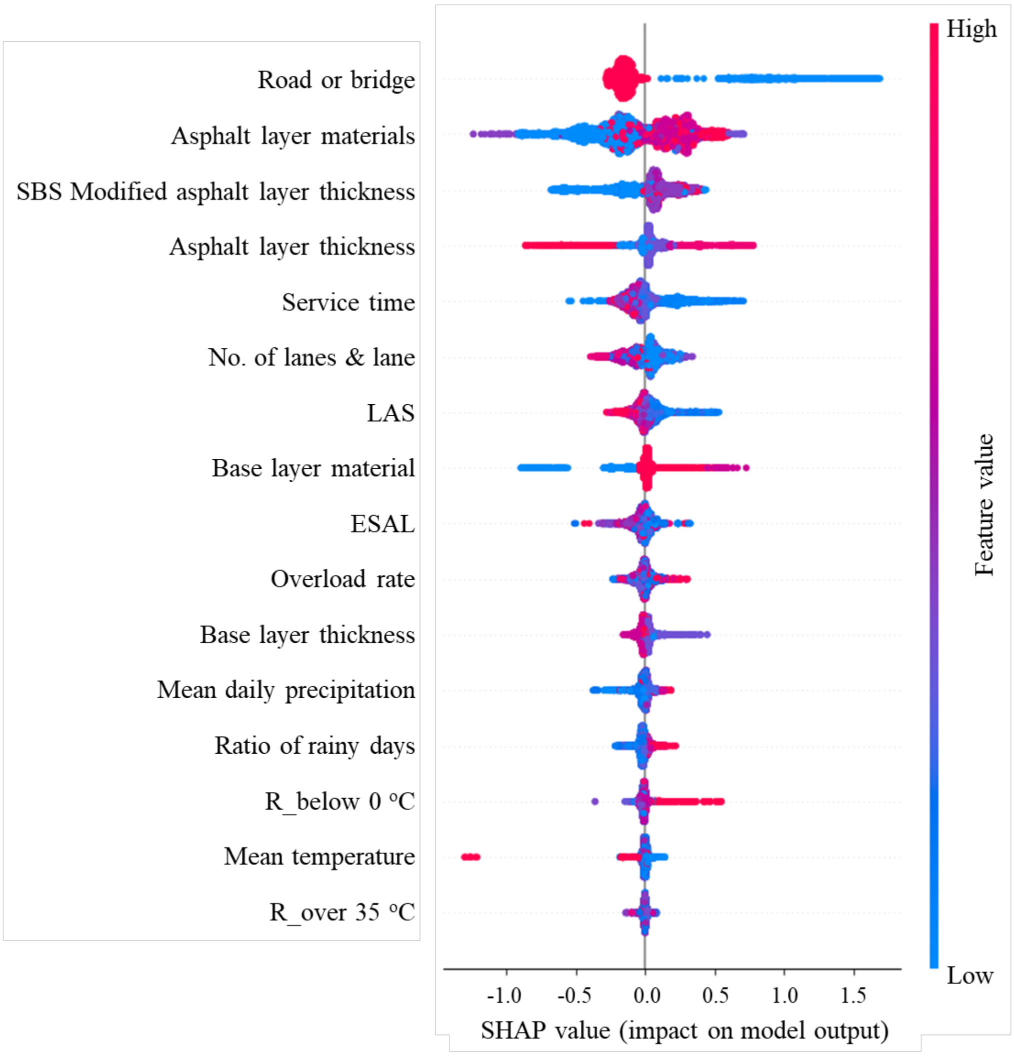

Figure 8. SHAP summary plot.

Figure 9 shows a scatter plot of SHAP values versus LAS index values for all samples in the dataset. It implies the effect of the LAS index on the model output throughout the whole dataset. As SHAP value represents the contribution of a feature to the change in the model output, the plot below depicts the change in TCEI values as the LAS index changes. A significant negative correlation can be observed in Figure 9. When the LAS index is less than one, the SHAP value tends to increase slightly with decreasing LAS, implying that a lower LAS index may improve the cracking performance of the pavement. When the LAS index is greater than one, the SHAP value decreases sharply with increasing LAS, indicating that early heavy traffic loading will significantly jeopardize the long-term cracking performance of the pavement.

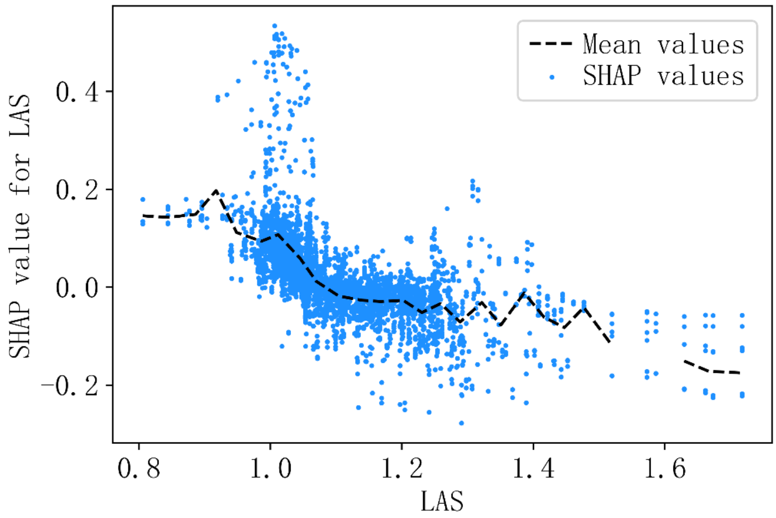

Figure 9. SHAP dependency plot for the LAS index.

The vertical dispersion in Figure 9 indicates the interactions of the LAS index with other features. To illustrate these interactions more clearly, the interacting variables and LAS index were first divided into groups. The vertical distribution of SHAP values for each group is then plotted using a box plot, as shown in Figure 10. The bottom half of Figure 10 is a line graph of the mean SHAP values, corresponding to the positions of the diamond symbols in the top half of Figure 10. It can be found that the effect of LAS index on the pavement cracking condition is greater for the road sections with relatively long service time and thin SBS modified asphalt layers. In other words, segments with longer service time were more sensitive to the traffic loading sequence. The modification of asphalt mixtures may mitigate the adverse impacts of heavy traffic loads in early stages.

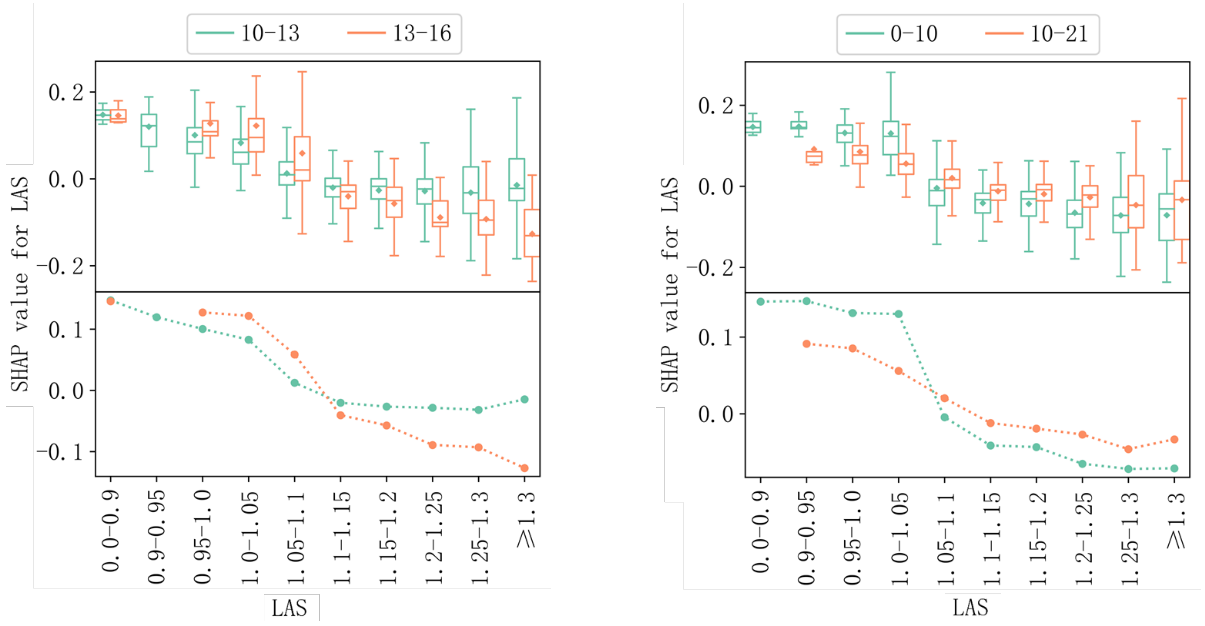

(a) (b)

Figure 10. Interaction effects between the LAS index and (a) service time and (b) SBS modified asphalt layer thickness.

4.2 Investigation of the loading sequence effect in laboratory

4.2.1 Fatigue curves of the two-block SCB test

Figure 11 illustrates the fatigue curves obtained in the SCB constant amplitude fatigue test at two stress ratios and in the two-block SCB test at two loading sequences. The vertical deformation curves of SCB specimens exhibit three stages under constant amplitude cyclic loading conditions: firstly, they accumulate rapidly with increasing loading cycles, then they grow steadily at an almost constant rate, and finally they accelerate in a non-linear mode until specimen failure. The fatigue failure criterion was the inflection point of the secondary and tertiary stage. It can be found that, in the first block, the deformation curves of the two-block SCB test and the SCB constant amplitude test at the same stress ratio almost overlap. In the second block, the deformation curves with loading sequences of σ_{high}-σ_{low} and σ_{low}-σ_{high} have much lower and higher growth rates than those with loading sequences of σ_{high} and

σ_{low}, respectively.

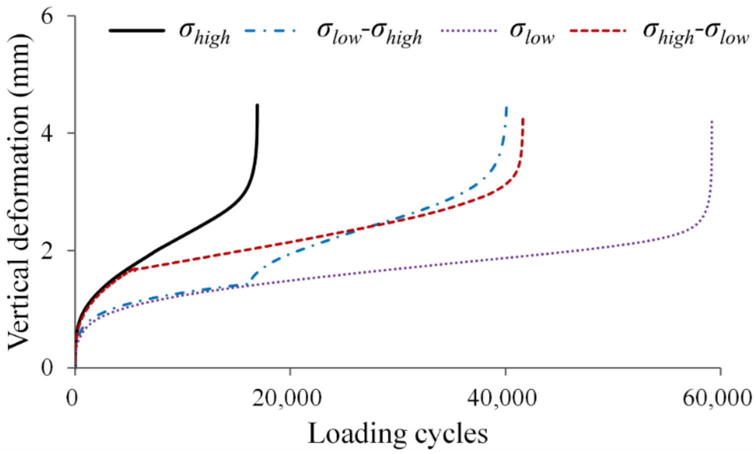

Figure 11. Fatigue curves of asphalt mixture specimens under different loading conditions.

4.2.2 Non-linear fatigue damage accumulation

In the two-block SCB fatigue test, applying N_1 cycles with a stress amplitude of σ_1 to specimen with a corresponding fatigue life endurance of $N_{f\sigma 1}$, is equivalent to consuming $N_1/N_{f\sigma 1}$ of the fatigue resistance (Schijve, 2009). This assumption also holds for the second block, so the accumulated damage variable (D_{sum}) was defined as the sum of $N_1/N_{f\sigma 1}$ and $N_2/N_{f\sigma 2}$. Table 4 presents the D_{sum} values of asphalt mixture specimens under two different loading sequences. According to the classic Miner's rule, D_{sum} should be equal to one under the linear cumulative damage hypothesis. However, the D_{sum} values of both loading sequences are not equal to one, suggesting that the asphalt mixture presents a non-linear fatigue damage accumulation characteristic. The D_{sum} value is less than one when the loading sequence is σ_{high}-σ_{low}, otherwise, the D_{sum} value is greater than one. This implies that a σ_{low}-σ_{high} sequence with D_{sum} greater than one may prolong the longevity and delay the crack propagation of asphalt mixtures. The results of the laboratory tests were consistent with the field validation results, which further demonstrated the effect of loading sequence on the cracking performance of asphalt pavements.

Table 4 D_{sum} of the asphalt mixture under two loading sequences.

Loading sequence	N_1	N_2	$N_{f\sigma 1}$	$N_{f\sigma 2}$	D_{sum}
σ_{high}-σ_{low}	5,080	36,563	18,502	56,722	0.918
σ_{low}-σ_{high}	17,751	27,124	56,722	18,502	1.902

4.3 Discussion

By combining the results of field and laboratory investigations, it can be concluded that a light-to-heavy loading sequence could prolong pavement service life, whereas a heavy-to-light sequence is detrimental to pavement cracking performance and may shorten the fatigue life of asphalt mixtures. Both field and laboratory results indicate that transport agencies need develop effective policies to prohibit the concentration of heavy traffic loads on individual road segments in the early stages of pavement service (i.e., after new construction or maintenance). Moreover, for long-term pavement cracking performance, the effect of loading sequence is more significant than the number of loading repetitions and overload rate. Its negative effects can be further exacerbated by longer service time and thinner modified asphalt layers. Hence, more attentions should be paid to segments with high LAS values, long service time, and thin modified asphalt layers to ensure timely maintenance.

5 Conclusions

In this study, the traffic loading sequence effect on the cracking performance of semi-rigid base asphalt pavements was investigated from both field and laboratory perspectives. Field validation was performed by applying simple graphic displays and advanced ML techniques to extract useful information from field pavement performance data. The two-block SCB tests were then conducted to further validate the loading sequence effects on the non-linear fatigue damage accumulation of asphalt mixtures.

A load amplitude sequence (LAS) index, built upon the variation of axle overload rates over the analysis period, was proposed and proved to be effective in characterizing the traffic loading sequence of in-service asphalt pavements. The graphic displays of the field pavement performance evolution under various combinations of LAS and ESAL levels demonstrate that a larger LAS value would increase the deterioration rate of pavement transverse cracking.

Both the ANN and RFR models have a relatively high accuracy, with the RFR model marginally outperforming the ANN model. The incorporation of the LAS index slightly improved the performance of the two models. The LAS index ranks high in the importance plot of the RFR model and is even more important than the other two traffic-related variables, indicating that the loading sequence has a significant impact on the prediction and development of pavement cracking conditions. The SHAP value analysis confirms that the heavier traffic loads in early stages are detrimental to the long-term pavement cracking performance. Moreover, this effect will be further exacerbated for pavement segments with longer service time or thinner SBS modified asphalt layers.

The D_{sum} values of asphalt mixtures under the loading sequence of σ_{high}-σ_{low} and σ_{low}-σ_{high} are greater and less than one, respectively, indicating that loading sequence starting with a higher stress may shorten the fatigue life of the asphalt mixture. In contrast, a light-to-heavy loading sequence would prolong the longevity of the asphalt pavement, which is consistent with the field validation results.

Finally, despite the contributions of this study, there are still some limitations that could be addressed in future work. For example, more complex load amplitude sequence indexes can be developed to characterize the entire time series of field traffic loads. Accordingly, more loading conditions may be considered in the variable amplitude fatigue test to prompt the better understanding of the non-linear fatigue damage accumulation of asphalt mixture.

Acknowledgements

This study was conducted under the support of the Research Institute for Sustainable Urban Development (RISUD) at the Hong Kong Polytechnic University. In addition, the data used in this research were collected from the Pavement Management System in Jiangsu province, China. The engineers and researchers who established the system and collected the data are also acknowledged for their contribution.

Disclosure statement

No potential conflict of interest was reported by the authors.

Reference

AASHTO, 1993. Guide for design of pavement structures. American Association of State Highway and Transportation Officials, Washington, DC.

Abaza, K.A., 2016. Back-calculation of transition probabilities for markovian-based pavement performance prediction models. International Journal of Pavement Engineering, 17 (3), 253-264.

Azari, H. & Mohseni, A., 2013. Permanent deformation characterization of asphalt mixtures by using incremental repeated load testing. Transportation research record, 2373 (1), 134-142.

Azari, H., Mohseni, A., Steger, R. & Muncy, D., 2021. Feasibility of using mastic for performance grading in place of extraction using sps10 mixtures. Transportation Research Record, 2675 (2), 1-14.

Chen, H., Zhang, Y. & Bahia, H.U., 2021. The role of binders in mixture cracking resistance measured by ideal-ct test. International Journal of Fatigue, 142, 105947.

Di Benedetto, H., Nguyen, Q.T. & Sauzéat, C., 2011. Nonlinearity, heating, fatigue and thixotropy during cyclic loading of asphalt mixtures. Road Materials and Pavement Design, 12 (1), 129-158.

Dong, N., Ni, F., Li, S., Jiang, J. & Zhao, Z., 2018. Characterization of permanent deformation performance of asphalt mixture by multi-sequenced repeated load test. Construction & building materials, 180, 425-436.

Dong, Q., Zhao, X., Chen, X., Ma, X. & Cui, X., 2021. Long-term mechanical properties of in situ semi-rigid base materials. Road Materials and Pavement Design, 22 (7), 1692-1707.

Gholamy, A., Kreinovich, V. & Kosheleva, O., 2018. Why 70/30 or 80/20 relation between training and testing sets: A pedagogical explanation.

Guler, S.I. & Madanat, S., 2011. Axle load power for pavement fatigue cracking: Empirical estimation and policy implications. Transportation research record, 2225 (1), 21-24.

Guo, F., Zhao, X., Gregory, J. & Kirchain, R., 2022. A weighted multi-output neural network model for the prediction of rigid pavement deterioration. International Journal of Pavement Engineering, 23 (8), 2631-2643.

Guo, R., Fu, D. & Sollazzo, G., 2021. An ensemble learning model for asphalt pavement performance prediction based on gradient boosting decision tree. International Journal of Pavement Engineering, 1-14.

Haider, S.W. & Harichandran, R.S., 2009. Effect of axle load spectrum characteristics on flexible pavement performance. Transportation research record, 2095 (1), 101-114.

Hu, W., Shu, X. & Huang, B., 2019. Sustainability innovations in transportation infrastructure: An overview of the special volume on sustainable road paving. Journal of Cleaner Production, 235, 369-377.

Jiang, J., Ni, F., Gao, L. & Lou, S., 2016. Developing an optional multiple repeated load test to evaluate permanent deformation of asphalt mixtures based on axle load spectrum. Construction & building materials, 122, 254-263.

Jiang, J., Ni, F., Dong, Q., Zhao, Y. & Xu, K., 2018. Fatigue damage model of stone matrix asphalt with polymer modified binder based on tensile strain evolution and residual strength degradation using digital image correlation methods. Measurement, 123, 30-38.

Karlaftis, A.G. & Badr, A., 2015. Predicting asphalt pavement crack initiation following rehabilitation treatments. Transportation Research Part C: Emerging Technologies, 55, 510-517.

Kim, D. & Kim, Y.R., 2017. Development of stress sweep rutting (ssr) test for permanent deformation characterization of asphalt mixture. Construction and Building Materials, 154, 373-383.

Lundberg, S.M. & Lee, S.-I., 2017. A unified approach to interpreting model predictionsed.^eds. Proceedings of the 31st international conference on neural information processing systems, 4768-4777.

Ministry of Transport of the People's Republic of China, 2016. Road management regulations for the movement of over-limited transport vehicles (Ministry of Transport Order No. 62 of 2016).

Pais, J.C., Amorim, S.I. & Minhoto, M.J., 2013. Impact of traffic overload on road pavement performance. Journal of transportation Engineering, 139 (9), 873-879.

Pedregosa, F., Varoquaux, G., Gramfort, A., Michel, V., Thirion, B., Grisel, O., Blondel, M., Prettenhofer, P., Weiss, R. & Dubourg, V., 2011. Scikit-learn: Machine learning in python. the Journal of machine Learning research, 12, 2825-2830.

Prozzi, J. & Madanat, S., 2004. Development of pavement performance models by combining experimental and field data. Journal of Infrastructure Systems, 10 (1), 9-22.

Santos, J., Ferreira, A. & Flintsch, G., 2017. A multi-objective optimization-based pavement management decision-support system for enhancing pavement sustainability. Journal of Cleaner Production, 164, 1380-1393.

Schijve, J., 2009. Fatigue of structures and materials: Springer.

Solatifar, N. & Lavasani, S.M., 2020. Development of an artificial neural network model for asphalt pavement deterioration using ltpp data. Journal of Rehabilitation in Civil Engineering, 8 (1), 121-132.

Timm, D.H., Tisdale, S.M. & Turochy, R.E., 2005. Axle load spectra characterization by mixed distribution modeling. Journal of Transportation Engineering, 131 (2), 83-88.

Tran, N.H. & Hall, K.D., 2007. Development and influence of statewide axle load spectra on flexible pavement performance. Transportation Research Record, 2037 (1), 106-114.

Van Rossum, G. & Drake, F.L., 2009. Python 3 Reference Manual. Scotts Valley, CA: CreateSpace.

Wang, X., Gu, X., Dong, Q., Wu, J. & Jiang, J., 2018. Evaluation of permanent deformation of multilayer porous asphalt courses using an advanced multiply-repeated load test. Construction and Building Materials, 160, 19-29.

Wang, Y.D., Underwood, B.S. & Kim, Y.R., 2022. Development of a fatigue index parameter, sapp, for asphalt mixes using viscoelastic continuum damage theory. International Journal of Pavement Engineering, 23 (2), 438-452.

Yao, L., Dong, Q., Jiang, J. & Ni, F., 2019. Establishment of prediction models of asphalt pavement performance based on a novel data calibration method and neural network. Transportation Research Record, 2673 (1), 66-82.

Yao, L., Dong, Q., Jiang, J. & Ni, F., 2020. Deep reinforcement learning for long-term pavement maintenance planning. Computer-Aided Civil and Infrastructure Engineering, 35 (11), 1230-1245.

Yao, L., Leng, Z., Jiang, J. & Ni, F., 2021. Modelling of pavement performance evolution considering uncertainty and interpretability: A machine learning based framework. International Journal of Pavement Engineering, 1-16.

Yuan, R., Li, H., Huang, H.-Z., Zhu, S.-P. & Gao, H., 2015. A nonlinear fatigue damage accumulation model considering strength degradation and its applications to fatigue reliability analysis. International Journal of Damage Mechanics, 24 (5), 646-662.

Zang, G., Sun, L., Chen, Z. & Li, L., 2018. A nondestructive evaluation method for semi-rigid base cracking condition of asphalt pavement. Construction and Building Materials, 162, 892-897.

Zhao, Z., Jiang, J., Ni, F., Dong, Q., Ding, J. & Ma, X., 2020. Factors affecting the rutting resistance of asphalt pavement based on the field cores using multi-sequenced repeated loading test. Construction & building materials, 253, 118902.

Zhou, L., Ni, F. & Leng, Z., 2014. Development of an asphalt pavement distress evaluation method for freeways in china. International Journal of Pavement Research & Technology, 7 (2).

Zhou, L., Ni, F. & Zhao, Y., 2010. Evaluation method for transverse cracking in asphalt pavements on freeways. Transportation research record, 2153 (1), 97-105.

Zhu, S.P., Hao, Y.Z., De Oliveira Correia, J.A., Lesiuk, G. & De Jesus, A.M., 2019. Nonlinear fatigue damage accumulation and life prediction of metals: A comparative study. Fatigue & Fracture of Engineering Materials & Structures, 42 (6), 1271-1282.